CHEMICAL ENGINEERING TRANSACTIONS
VOL. 41, 2014
A publication of AIDIC
The Italian Association of Chemical Engineering
www.aidic.it/cet
Guest Editors: Simonetta Palmas, Michele Mascia, Annalisa Vacca

ISBN 978-88-95608-32-7; **ISSN** 2283-9216
DOI: 10.3303/CET1441052

MoO_2 Synthesis for LIBs

Maria Sarno, Anna Garamella, Claudia Cirillo*, Paolo Ciambelli

Department of Industrial Engineering and Centre NANO_MATES, University of Salerno
Via Giovanni Paolo II ,132 - 84084 Fisciano (SA), Italy
clcirillo@unisa.it

MoO_2/few layer graphene nanostructures have been prepared via a solvent free easily controllable and scalable process, consisting in the thermolysis of a suitable precursors in presence of few layer graphene (FLG), followed by an annealing. FLG has been prepared by a liquid phase exfoliation in N-methylpyrrolidone (NMP) of graphite, producing unoxidized graphene by a non-covalent, solution-phase method. The hybrid material consists in MoO_2 nanostructures on a graphene support anchoring and covering the nanoparticles. The MoO_2 nanocrystals result intimately mixed and trapped by the FLG that works as a highly flexible and conductive matrix for good contact between them. In particular, the precursor decomposition was promoted in the temperature range 25-800°C, followed by an annealing to obtain high quality material. The synthesis product was carefully characterized by Raman Spectroscopy, Scanning (SEM) and Transmission (TEM-EDS) Electron Microscopy, thermogravimetric analysis (TG-DTG-MS) and X-ray diffraction (XRD). The synthesis process was monitored with a mass spectrometer to follow the evolution of the reactions.

1. Introduction

The research on lithium ion batteries (LIBs) has recently attracted a lot of interest in the field of fundamental study and applied research. In particular, MoO_2 has recently received much attention, and has been considered as a promising anode material in LIBs, in substitution of carbon materials requiring six carbon atoms to accommodate one Li ion (Whittingham, 2004), because of its low electrical resistivity, high electrochemical activity, high stability, and high theoretical capacity (Tang et al., 2012). Even if bulk MoO_2 has low storage capacity, the morphological properties are found to play an important role in their lithium-intercalation activity and cycling stability. In the last few years, a wide variety of approaches have been pursued to synthesize different nanostructured MoO_2, finding that they lead to different diffusion lengths and different stored amounts of Li+. Ordered mesoporous MoO_2 materials (Shi et al.,2009), hollow core–shell MoO_2 microspheres (Lei et al., 2012) and MoO_2 nanorods (Zheng et al., 2010) have been extensively investigated. However, in the metal-oxide electrodes pulverization occurs during the volume change, leading to a rapid decay in capacity and limiting the potential use (Cabana et al., 2010). Therefore, developing new synthetic strategies to fabricate high-performance metal oxide electrode materials, with both large reversible capacity and long cycle life, still remains a great challenge to chemists and materials scientists. Electrodes taking advantage of nanometer size materials, and of a second stabilizing material, exhibit intriguing properties. The use of carbon can have several functions, including: (i) maintaining the integrity of particles, (ii) increasing the electronic and thermal conductivity of electrodes, and (iii) stabilizing the conductive network. In most conventional electrodes, metal oxide nanoparticles are directly mixed with a carbon additive and a binder to help maintain electrical conductivity. No polymer binder is required in (Ban et al., 2010), where, through an hydrothermal process followed by a filtration, a single-walled carbon nanotubes/MoO_2 composite were found to have high rate capability and high capacity. Carbon coating has been widely used to create a conductive layer enclosing the active materials (Zhang et al., 2008). On the other hand, when it covers the active materials surface tightly, difficulties to release the large strain from the volume expansion can be registered. Sun et al. (Sun et al., 2011) reported the fabrication of hierarchical MoO_2/graphene nanoarchitectures through a solution-based method, starting from graphene oxide (GO) prepared using a modified Hummer method (Hummers and Offeman, 1958)

Please cite this article as: Sarno M., Garamella A., Cirillo C., Ciambelli P., 2014, Moo2 synthesis for libs, Chemical Engineering Transactions, 41, 307-312 DOI: 10.3303/CET1441052

and phosphomolybdic acid, combined with a subsequent reduction process also to improve the GO order. They found that the as-formed MoO_2/graphene nanohybrid exhibited highly reversible capacity, excellent cyclic performance, and good rate capability. They use graphene for its superior electrical conductivity, large surface area, structural flexibility, and chemical stability.

Here we report the synthesis of MoO_2 nanostructure/few layer graphene composites, the MoO_2 nanostructures were prepared by a simple and scalable process, consisting in a thermolysis of a suitable precursors followed by an annealing. The synthesis process is very versatile, permitting to prepare MoO_2 nanostructure on a graphene support, anchoring and covering the nanoparticles and working as a highly flexible and conductive matrix for good contact between them. Few layers graphene (FLG), used for this work, was prepared by a liquid phase exfoliation in N-methylpyrrolidone (NMP) (Hernandez et al., 2008) of graphite, producing unoxidized graphene by a non-covalent, solution-phase method. In particular, MoO_2 nanocrystals were prepared via a solvent free thermolysis of ammonium molybdate ($(NH_4)_6Mo_7O_{24}{\cdot}4H_2O$) in presence of graphene, in a continuous flow microreactor fed by an inert flow (Giubileo et al., 2012; Sarno et al., 2012; Sarno et al., 2013). The syntheses were monitored with a mass spectrometer to follow the evolution of the reactions. For the characterization the combined use of different techniques such as micro-Raman Spectroscopy, Scanning Electron Microscopy (SEM), Transmission Electron Microscopy – Energy dispersive X-ray spectroscopy (TEM-EDS), thermogravimetric analysis coupled with a mass spectrometer (TG-DTG-MS), X-ray diffraction (XRD), were employed.

2. Experimental

MoO_2 nanocrystals were prepared by thermolysis of ammonium molybdate ($(NH_4)_6Mo_7O_{24}{\cdot}4H_2O$) (Sigma Aldrich) in a continuous flow microreactor fed by nitrogen (200 cm^3(STP)/min). FLG were obtained by a sonication of graphite in N-methylpyrrolidone (NMP, spectrophotometric grade> 99.0%) (cylindrical vial, 10-25 ml solvent) at a concentration of 10 mg/ml for 1 h at the maximum power of ultrasound (Hielscher UP 400S). FLG were recovered by vacuum filtration of the supernatant solution obtained after a suitable centrifugation (the supernatant contains about the 30 wt% of the original graphite -TG evaluation, not reported here), onto: porous alumina membranes (pore size: 20 nm). For the MoO_2/FLG composite (MoO_2-1), ammonium molybdate and FLG were sonicated in water for 30 min to obtain a loading of 30 wt.% total Mo metal content, after drying at 130°C, the powder mixture was loaded in the reactor and heated from room temperature to 800°C, and then annealed at that temperature for 2 h in the presence of a 0.5 vol.% of oxygen in nitrogen flow). All the samples obtained were characterized by the combined use of different techniques. Transmission electron microscopy (TEM) images were acquired using a FEI Tecnai electron microscope operated at 200 KV with a LaB6 filament as the source of electrons, equipped with an EDX probe. Scanning electron microscopy (SEM) images were obtained with a LEO 1525 microscope. Raman spectra were obtained at room temperature with a micro-Raman spectrometer Renishaw inVia with a 514 nm excitation wavelength (laser power 30 mW) in the range 100-3000 cm^{-1}. Optical images were collected with a Leica DMLM optical microscope connected on-line with the Raman instrument. For all the sample about 40 measurements have been carried out. The laser spot diameter was about 10 μm. XRD measurements were performed with a Bruker D8 X-ray diffractometer using CuK_α radiation. Thermogravimetric analysis (TG-DTG) at a 10 K/min heating rate in flowing air was performed with a SDTQ 500 Analyzer (TA Instruments) coupled with a mass spectrometer.

3. Results and discussion

Figure 1 shows the representative SEM images for the MoO_2/graphene product, at increasing magnifications. The sample is constituted of large aggregates consisting of smaller particles, few microns in size, of various shapes and with a rough surface.

Figure 2a, 2b, 2c show three bright-field TEM images, at different magnifications, of FLG flakes typically observed. The TEM images reveal the presence of flakes of graphene and multilayer graphene sheets in the sample. They have lateral sizes of few micrometres, in many cases the sheet edges tend to scroll and fold slightly. The corresponding electron diffraction pattern (Figure 2g) confirms the carbon sp2 nature of the sheets. In particular, in the insert of Figure 2b and in Figure 2c, 1 layer and 10 layers, with the interplanar spacing of 0.33 nm, corresponding to the separation between (002) lattice planes of graphite, can be counted, respectively. By analyzing a large number of TEM images, paying attention to the uniformity of the flake edges and from a statistic analysis of over 200 objects, we generated flake thickness statistics as shown in Figure 2d (normalized on 100 objects). From these data we estimated the number fraction of monolayer graphene (number of monolayers/total number of flakes observed) in NMP dispersions as 22%. This corresponds to a solution-phase monolayer mass fraction (mass of all

monolayers/mass of all flakes observed) of 5.5 wt%, leading to an overall yield of 1.8 wt. % (the supernatant contains about the 30 wt% of the original graphite)

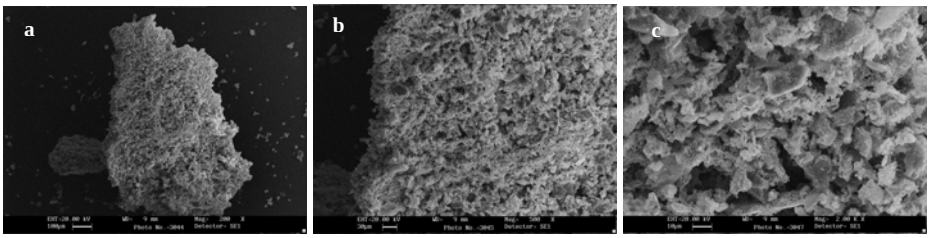

Figure 1. SEM images of the MoO2-1 hybrid at different magnifications. Scale bar: 100μm (a), 30μm (b) and 10μm (c).

TEM investigations carried out, to provide further insights into the morphology, on the resulting MoO_2/FLG nanostructures, are reported in Figure 2e, 2f, 2i, 2l, at increasing magnifications. Figure 2e shows a typical TEM image at low magnification for the product. It is clearly observed that the rough particles, shown in the SEM images, comprise numerous primary MoO_2 nanocrystals (10-90 nm, Figure 2f) intimately mixed and trapped by the FLG (Figure 2i and 2l). It is worth to notice that MoO_2-1 but annealing is constituted of large particles, hundred nanometers in size, and FLG. The selected area electron diffraction (SAED) rings reveal the polycrystalline nature of the sample (Figure 2h). High resolution TEM (HRTEM) images taken from two individual MoO_2 nanocrystals are shown in Figure 2m and 2n. The periodic fringe spacing of ~1.7 Å, ~1.8 Å and ~3.4 Å agree well with the interplanar spacing between the {220}, $\{1\bar{2}1\}$ and {110} planes of monoclinic MoO_2, respectively.

In Figure 3a the thermogravimetric (TG-DTG) and temperature profiles, during the test simulating the MoO_2/FLG hybrid synthesis conditions, are reported as function of time. The weight loss appearing below 300°C, arising from the decomposition of ammonium molybdate (as clearly indicated by the corresponding total ion current (TIC) of the most intense mass fragments peaks: m/z = 15, 16, 17 from NH_3); MoO_3 is thus formed (Chen et al., 2013). At about 500°C a CO release starts, with a maximum at 643°C, due to the reduction, in presence of carbon, from MoO_3 to MoO_2. The TG residue at 800°C, 84.55 wt.%, results compatible with the starting amount of FLG (also taking into account the low amount of carbon reacting with oxygen to give MoO_2) and the MoO_2 content. It is worth to notice that during the annealing time, due to the few percent of oxygen fed to the reactor, the oxidation of a 2 wt.% of carbon takes place. We have verified that for the unsupported sample, the sublimation of MoO_3 occurred at around 800°C, as previously reported (Chen et al., 2013). According to Delporte et al. (Delporte et al., 1995), the MoO_2 formation goes through the oxygen removal from the MoO_3 structure, and if a sufficient number of oxygen vacancies were generated the lattice can easily rearrange from a corner-sharing to an edge-sharing octahedral structure by a crystallographic shear-plane process. A number of studies (Frauwallner et al., 2011; Delporte et al., 1995) have been performed to follow the evolution of the MoO_3+vacancies intermediate state, in different reduction (H_2 atmosphere)-carburization (hydrocarbons atmosphere) conditions, showing that, MoO_2 or, by incorporation of carbon atoms, Mo_2C can be produced. In our experimental conditions, the formation of MoO_2 is allowed by the presence of FLG, which react with oxygen from MoO_3, to give CO, as previously reported (Chen et al., 2013). On the other hand, Chen et al. report that, in presence of solid carbon source, a temperature of 800°C is sufficient to determine the beginning of the formation of Mo_2C, indeed the incorporation of C is most likely to occur in two possible ways (Frauwallner et al., 2011), either by filling anionic vacancies, without going through the MoO_2 formation, or by direct exchange with an oxygen atom. In our case, form 800°C and during the annealing time, the few trace of oxygen present in the reactor feed combines with carbon, permitting to preserve the MoO_2 crystallographic structure.

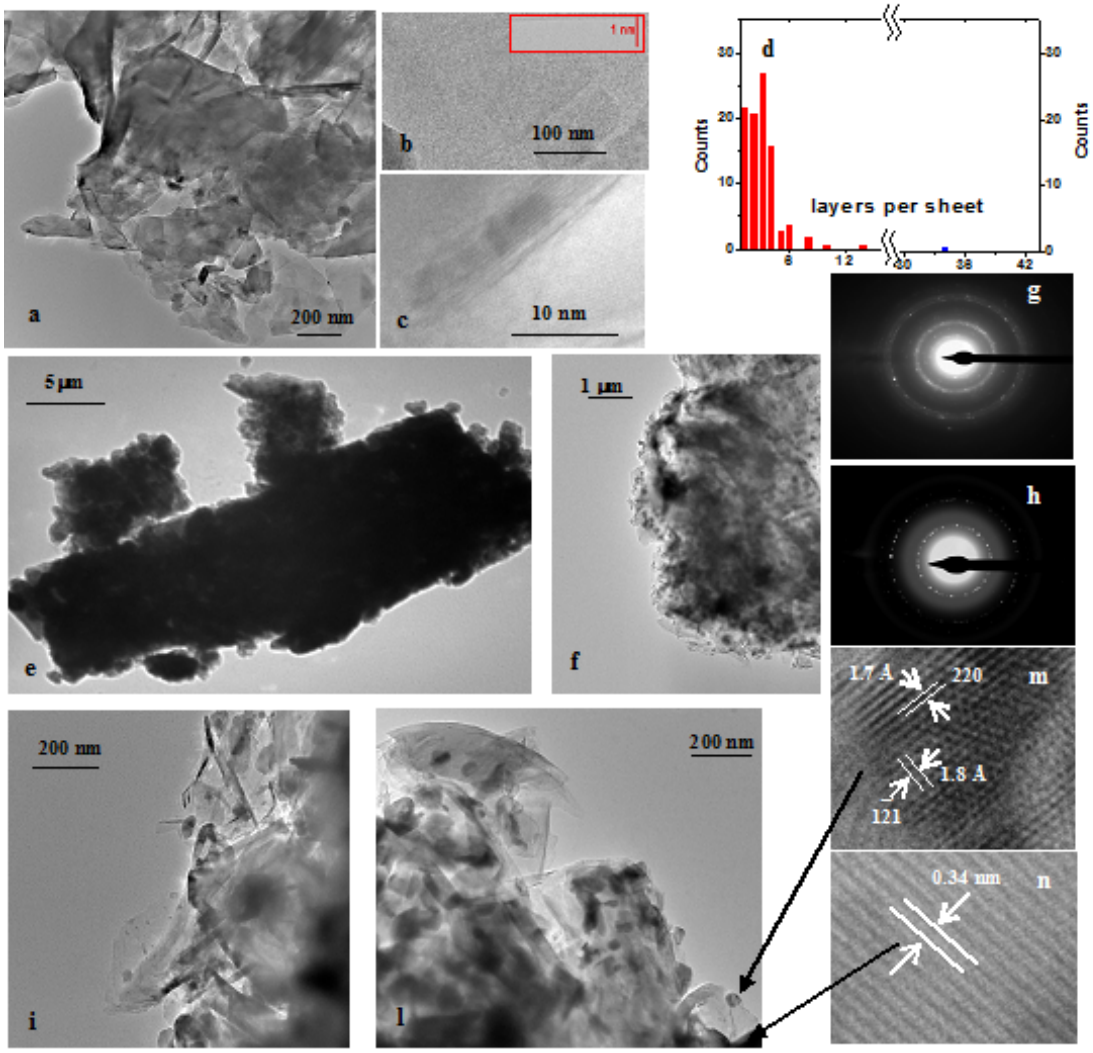

Figure 2. TEM images of FLG at increasing magnification (a, b, c). Histogram of the number of layer per sheet (d). TEM images of MoO2-1 (e, f, i, l). HRTEM image of MoO_2 nanoparticles indicated by arrows (m,n). SAED pattern of FLG (g). SAED pattern of MoO2 (h).

Figure 3b shows the X-ray diffraction (XRD) patterns: for the physical mixture of the precursor and graphene; for the final MoO_2-graphene product (MoO_2-1), prepared by annealing the Mo-precursor/graphene intermediate at 800°C for 2h; and for a sample obtained in the same conditions but annealing. For both the last two samples, all the diffraction peaks are readily indexed to a pure monoclinic phase. No characteristic peaks from MoO_3 are observed as well as other molybdenum oxides. The sample not annealed is characterized by a lower degree of order, as evidenced by the resolution and sharpness of the various peaks. After the annealing time the intensity of the (110) peak of MoO_2 increased if compared with the (002) peak of FLG, also indicating the increased order for the annealed sample. Meanwhile, the stoichiometry of the MoO_2 nanoparticles, in MoO_2-1, was confirmed with energy dispersive TEM based X-ray spectroscopy (EDS) (Figure 3c). Figure 4 shows the Raman spectrum of MoO_2-1, in order to provide a better analysis, the spectrum was plotted in two regions: 200-900 cm^{-1}, in which MoO_2 spectrum is visible; and 1000-3000 cm^{-1} for the typical Raman bands of FLG. For both the spectra the y axes are arbitrary scales, the spectra are not normalized, being the intensity of the MoO_2 spectrum amplified. In the high wavelength range the two most intense features are the G peak at ~1570 $cm^{-1}$and a band at ~2700 cm^{-1}, named 2D, since it is the second most prominent peak always observed in graphite samples (Casiraghi et al., 2005). The G peak is due to the doubly degenerate zone center E_{2g} mode (Ferrari et al., 2003), while the 2D band is the second order of zone-boundary phonons. Such phonons give rise to a peak at about

1350 cm^{-1} due to disorder or edge in graphite, called D band (Ferrari et al., 2003). The G band is cantered at 1565 cm^{-1}, the 2D band is not the typical of graphite consisting of the two components 2D1 and 2D2, the second with an highest intensity than the first (Meyer et al., 2007), has a flat apex and can be easily deconvoluted with almost two peaks. A broad D-band can be seen, it has been demonstrated (Hernandez et al., 2008) that the sonication exfoliation process does not introduce significant structural defect, on the other hand our laser spot diameter was 10 μm, a value higher than the size of the obtained flakes suggesting the presence of edges within the analyzed area.

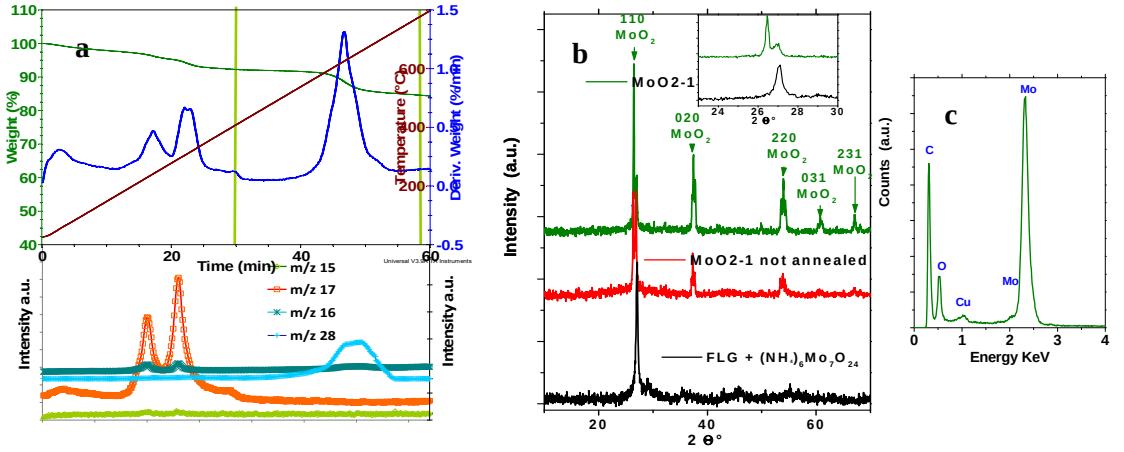

Figure 3. TG-DTG profiles, during the test simulating the MoO_2-1 synthesis conditions, and the corresponding TIC (a). XRD diffraction patterns of the precursor, of a samples not annealed and of MoO_2-1 (b). EDX of the MoO_2-1 hybrid (c).

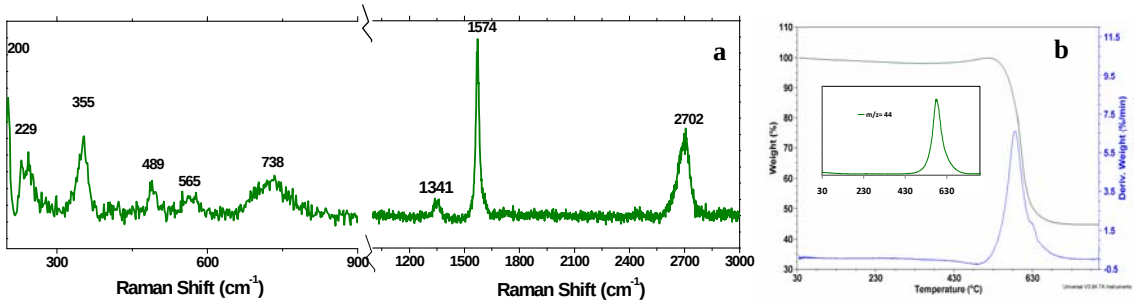

Figure 4. Raman spectrum of MoO_2-1 in the range 200-3000 cm^{-1} (a). TG-DTG curves of the as prepared MoO_2-1 hybrid (b).

Thermogravimetic analysis of MoO_2-1 was performed in flowing air (Figure 4b), the weight change between 400 and 700°C is due to both the oxidation of MoO_2 and the combustion of FLG (as confirmed by the mass fragments peak m/z = 44 form CO_2, see the Figure 5a insert). The theoretical value of weight increase from MoO_2 to MoO_3 is 12.5%; the FLG content in the hybrid is evaluated to be about 58 wt.% of the sample. This value agrees with the original FLG content in the precursor mixture accounting for the small weight loss of FLG observed during the MoO_2 annealing.

4. Conclusions

We have successfully demonstrated the preparation of MoO_2/FLG hybrid, , through a solvent free easily controllable and scalable process. The hybrid material consists in MoO_2 nanometer optimized size for Li-ion diffusion, on a few layer unoxidized graphene support anchoring and covering the nanoparticles. The MoO_2 nanocrystals result intimately mixed and trapped by the FLG that works as a highly flexible and conductive matrix for good contact between them. The synthesis results was a pure monoclinic MoO_2 phase, without impurities such as molybdenum oxides. The synthesis technique permits to obtain different degree of order materials, simply by increasing the annealing time, allowing to elucidate the material order effect on the performance of the electrodes.

References

Ban C., Wu Z., Gillaspie D. T., Chen L., Yan Y., Blackburn J. L., Dillon A. C., 2010, Nanostructured Fe3O4/SWNT Electrode: Binder-Free and High-Rate Li-Ion Anode, Adv. Mater. 22, E145-E149.

Cabana J., Monconduit L., Larcher D., Palacín M.R., 2010, Beyond Intercalation-Based Li-Ion Batteries: The State of the Art and Challenges of ElectrodeMaterials Reacting Through Conversion Reactions, Adv. Mater. 22, E170-E192.

Casiraghi C., Ferrari A.C., Robertson J., 2005, Raman spectroscopy of hydrogenated amorphous carbons, Phys. Rev. B 72, 085401 (14pp).

Chen W. F., Wang C.H., Sasaki K., Marinkovic N., Xu W., Muckerman J. T., Zhu Y., Adzic R.R., 2013, Highly Active, Durable, and Nanostructured Molybdenum Carbide Electrocatalysts for Hydrogen Production, Energy Environ. Sci. 6, 943-951.

Delporte P., Meunier F., Pham-Huu C., Venneguesb P., Ledoux M. J., Guille J., 1995, Physical charatreization of molybdenum oxycarbide catalyst: TEM, XRD and XPS, Catal. Today 23, 251-267.

Ferrari A.C., Rodil S.E., Robertson J., 2003, Interpretation of infrared and Raman spectra of amorphous carbon nitrides, Phys. Rev. B 67, 155306 (20pp).

Frauwallner M.L., López-Linares F., Lara-Romero J., Scott C.E., Ali V., Hernández E., Pereira-Almao P., 2011, Toluene hydrogenation at low temperature using a molybdenum carbide catalyst, Appl. Catal., A 394, 62-70.

Giubileo F., Di Bartolomeo A., Sarno M., Altavilla C., Santandrea S., Ciambelli P., Cucolo A.M., 2012, Field emission properties of as-grown multiwalled carbon nanotube films, Carbon 50, 163-169.

Hernandez Y., Nicolosi V., Lotya M., Blighe F.M., Sun Z., De S., McGovern I.T., Holland B., Byrne M., Gun'ko Y.K., Boland J.J., Niraj P., Duesberg G., Krishnamurthy S., Goodhue R., Hutchison J., Scardaci V., Ferrari A.C, Coleman J.N., 2008, High-yield production of graphene by liquid-phase exfoliation of graphite, Nat. Nanotechnol. 3, 563-568.

Hummers W. S., Offeman R. E., 1958, Preparation of Graphitic Oxide, J. Am. Chem. Soc. 80, 1339-1339.

Lei Y., Hu J., Liu H., Li J., 2012, Template-free synthesis of hollow core-shell MoO2 microspheres with high lithium-ion storage capacity, Mater. Lett. 68, 82-85.

Meyer J.C., Geim A. K., Katsnelson M. I., Novoselov K.S., Obergfell D., Roth S., Girit C., Zettl A., 2007, On the roughness of single- and bi-layer graphene membranes, Solid State Commun. 143, 101-109.

Sarno M., Cirillo C., Piscitelli R., Ciambelli P., 2013, A study of the key parameters, including the crucial role of H2 for uniform graphene growth on Ni foil, J. Mol. Catal. A: Chem. 366, 303-314.

Sarno M., Sannino D., Leone C., Ciambelli P., 2012, Evaluating the effects of operating conditions on the quantity, quality and catalyzed growth mechanisms of CNTs, J. Mol. Catal. A: Chem. 357, 26-38.

Shi Y., Guo B., Corr S. A., Shi Q., Hu Y.S., Heier K.R., Chen L., Seshadri R., Stucky G.D., 2009, Ordered mesoporous metallic MoO2 materials with highly reversible lithium storage capacity, Nano Lett. 9, 4215-4220.

Sun Y., Hu X., Luo W., Huang Y., 2011, Self-Assembled Hierarchical MoO2/Graphene Nanoarchitectures and Their Application as a High-Performance Anode Material for Lithium-Ion Batteries, A.C.S. Nano 5, 7100-7107.

Tang Q., Shan Z., Wang L., Qin X., 2012, MoO2-graphene nanocomposite as anode material for lithium-ion batteries, Electrochim. Acta 79, 148-153.

Whittingham M. S., 2004, Lithium Batteries and Cathode Materials, Chem. Rev. 104, 4271-4302.

Zhang W.M., Wu X. L., Hu J. S., Guo Y. G., Wan L. J., 2008, Carbon Coated Fe3O4 Nanospindles as a Superior Anode Material for Lithium-Ion Batteries, Adv. Funct. Mater. 18, 3941-3946.

Zheng L., Xu Y., Jin D., Xie Y., 2010, Well-aligned molybdenum oxide nanorods on metal substrates: solution-based synthesis and their electrochemical capacitor application, J. Mater. Chem. 20, 7135-7143.